STAT

CHARACTERISTICS OF THE MICROSTRUCTURE OF WIND IN THE LAYER OF THE ATMOSPHERE CLOSE TO THE GROUND"

author: A. M. Obukhov (Geophy Inst, Acad Sci USSR)

Source:

Izvestiya Akademii Nauk SSSR, Seriya Geofizicheskaya, No 3, 1951, pages 49-68

STAT

CHARACTERISTICS OF THE MICROSTRUCTURE OF THE WIND IN THE LOWEST ATMOSPHERIC LAYER

A. M. Obukhov

(Submitted by Academician A. N. Kolmogorov)

The methods of measuring the pulsations of wind velocity are described, and the results of research into the microstructure of the wind in the lowest atmospheric layer (up to 15 meters) are discussed. The results of direct measurements of the characteristics of atmospheric turbulence are compared with the deductions made from the theory of local isotropic turbulence. Experiments in the measurement of the vertical component of wind velocity and in the determination of the Reynolds stresses are described.

The tangible fields of meteorological magnitudes (the fields of wind velocities, temperature, moisture) are of a very complex structure, which is linked to the turbulent state of atmospheric motion. Meteorologists are familiar with the "external" manifestations of atmospheric turbulence, such as "virtual" friction, the transfer of heat and material admixtures. To account for these factors in theoretical research it is usual to introduce certain conventional coefficients of turbulent viscosity, turbulent heat conduction and diffusion.

In addition to these indirect methods of turbulence calculation the direct study of the turbulent pulsations and the investigation of the structure of the turbulent current in the conditions of the atmosphere are of considerable interest to the physics of the atmosphere. The importance of the study of the microstructure of meteorological fields in atmospheric acoustics, atmospheric optics, and also to the development of the theory of aerosol coagulation under natural conditions, is obvious.

The modern theory of the developed turbulent current, created by the efforts of Soviet scientists (A. A. Friedman, academician A. N. Kolmogorov and his school, academician L. D. Landau), points to a series of regularities in the structure of atmospheric turbulence which as yet have been little investigated experimentally.

This thesis presents the results of the measurements of the structural characteristics of atmospheric turbulence. The measurements were made with the aid of special apparatus designed by the author in collaboration with S. I. Krechmer of the Geophysical Institute, Academy of Sciences USSR. The factual data obtained on the structure of turbulence in the lowest atmospheric layer are in adequate agreement with the theory of local isotropic turbulence. This thesis also describes the tests for the measuring (registration) of the momentary values of the vertical wind velocity component for the purpose of deriving a method for the direct determination of turbulent friction intensity in the lowest atmospheric layer.

1. STRUCTURAL FUNCTION OF THE FIELD OF VELOCITIES IN A TURBULENT CURRENT

As far back as 1925, A. A. Friedman [1] suggested the utilization of the correlation between the momentary values of the elements of the hydrodynamic field at two points of the current as characteristics for the structure of the turbulent current. This method found wide application in experimental aerodynamics for the study of turbulence in wind tunnels. However, in applying this method to the solution of geophysical problems, a basic difficulty in the determination of the "mean" field of velocities, temperatures, and other atmospheric characteristics is encountered. This difficulty is linked to the known phenomenon of the "evolution of the level" of the geophysical fields, as a result of which our computations will depend substantially on the selection of the averaging period. The problem of the actual determination of the "averaged field" becomes simplified, if the method submitted by academician Kolmogorov in 1941 [2, 3] is used. This method consists in describing the structure of the turbulent current by means of statistical characteristics, relating not to the actual values of the field, but only to the differences of these values at two points of the current. If the two observation points are in the same macroscopic conditions (sufficiently close to each other, the underlying surface sufficiently homogeneous), the difference between the values of the current velocity or temperature is a statistically stable magnitude, whose mean value can, with sufficient accuracy, be considered as equal to zero. The mean range of the momentary values in the characteristics at two points of the current at a distance r from each other is the measure of the intensity of the perturbation of the scale, which is less than or comparable to r in value. The ratio of the mean square of the difference between the characteristics of the field at two points, to the distance between these points, is called the structural function of the given field.

Knowing the structural function of the field of velocities and of the field of temperatures furnishes definite data on the spectrum of turbulence and renders the solution of a series of concrete geophysical problems possible. As an example, we refer the reader to the works by V. A. Krasil'nikov [4, 5], who investigated the propagation of sound and light in a turbulent atmosphere, and to the work by M. I. Yudin [6] on the oscillations of a plane in flight. The concept of a structural function for the wind — the vectorial field — requires additional explanation. Let M_1 and M_2 be the points of observation. Let us introduce into the analysis magnitudes D_{ll} and D_{nn} :

$$\left.\begin{aligned} D_{ll} &= \overline{[(\Delta v)_l]^2}, \\ D_{nn} &= \overline{[(\Delta v)_n]^2}, \end{aligned}\right\} \qquad (1)$$

where $(\Delta v)_{\ell} = [v(M_2) - v(M_1)]_{\ell}$ is the vectorial projection of the difference in velocities in the direction of axis M_1M_2 (the base). $(\Delta v)_n$ is the projection of the same difference in a direction n, perpendicular to the direction of the base. In conformity with the A. N. Kolmogorov theory of local isotropy of the turbulent flow, magnitudes $D_{\ell\ell}(r)$ and $D_{nn}(r)$ can be considered as functions of distance r only (with r small by comparison with the external scale of turbulence), which functions are independent of the orientation of the base and of the special selection of the direction n in a plane, perpendicular to the base. We will call these functions $D_{\ell\ell}(r)$ and $D_{nn}(r)$, respectively, the longitudinal and transverse structural function of the field of velocities (the field of the wind). Under conditions of the atmosphere the "external scale" of turbulence can be considered to have a magnitude of the order of the path of coalescence, about 1/3 of the distance from the underlying surface (height).

The longitudinal and the transverse structural functions are linked by some equation which follows from the equation of continuity (see Kolmogorov [2]):

$$D_{nn}(r) = D_{\ell\ell} + \frac{r}{2}\,\frac{dD_{\ell\ell}}{dr}, \qquad (2)$$

whence it follows, in particular, that

$$D_{\ell\ell}(r) = \frac{2}{r^2} \int_0^r r\, D_{nn}(r)\, dr. \qquad (3)$$

As we will see below, in studying experimentally the structure of the field of the wind it is considerably more convenient (for technical reasons) to determine the transverse structural function, and not the longitudinal.

In our experiments we used a horizontal base, perpendicular to the direction of the wind, with Δv_n -- the projection of the difference of velocities in the direction of the basic current being measured. In subsequent text, for purposes of brevity, we will frequently refer to the structural function of the field of the wind, while having in mind the transverse structural function and the above indicated diagram of measurements. (For small distances, due to the local isotropy of the current, the selection of the direction of the base has no substantial significance. However, when using a horizontal base, the concept of the structural function retains its meaning not only for very small distances, but also for distances r, comparable with the observation altitude and even in excess of same, since the field of the wind over an adequately homogenous underlying surface can be considered statistically homogeneous and isotropic in a horizontal direction. It is obvious that with such an expanded comprehension of the concept of structural function we can compare the empirical data of local isotropic turbulence only for distances not in excess of the external turbulence scale.)

In accordance with the theoretical research by A. N. Kolmogorov and the author [2, 7, 8], the structural function of the field of velocities of a developed turbulent current, for distances r which are considerably in excess of the "internal scale of turbulence" η, determinable only by the mean energy dissipation ε and the viscosity of the environment ν, has the rather simple form

$$D_{nn}(r) = b^2 r^{2/3}, \qquad (4)$$

where b is the characteristic of the intensity of the micropulsations (the structural characteristic of the field of the wind).

For values of r considerably smaller than η, D_{nn} is proportional to the square of r. The internal scale of turbulence η, introduced into the theory of turbulence by A. N. Kolmogorov, characterizes the magnitude of the "laminary elements" in the turbulent current. In accordance with reference [7], we will use the determination of the internal scale of turbulence η_1, corresponding to the "point of discontinuity" of the structural function (this scale is distinguished only by the presence of a numerical factor, approximately equal to unity, from the scale η, introduced by A. N. Kolmogorov):

$$\eta_1 = \frac{5{,}035}{\sqrt{|S_1|}} \sqrt[4]{\frac{\nu^3}{\varepsilon}}, \qquad (5)$$

where S_1 is the numerical coefficient (the asymmetry of the distribution of the longitudinal component in the difference of velocities at closely located points). According to measurements taken by Townsend [9] in wind tunnel tests, $S_1 \approx 0.4$. This value, however, cannot be considered as finally established and cannot be used without reservations for all cases of turbulent motion. In conformity with formula (5) and with the direct measurement of the structural function of the field of velocities, as effected by Godecke [10], the scale η_1, is on the order of magnitude of several millimeters. The results of the measurement of the difference in velocities at a distance not less than two centimeters, as cited below, can, therefore, be considered as pertaining to "great" distances, and can be compared with the experimental values of the structural function [4].

The structural characteristic of the field of the wind b, in accordance with references [2, 3, 8] is linked directly with the mean value of energy dissipation :

$$b = C_1 \sqrt[3]{\varepsilon}. \qquad (6)$$

The numerical constant C_1 can be expressed by the Kolmogorov [3] constant C as follows:

$$C_1 = \sqrt{\frac{4}{3}}\, C,$$

and, as theoretically proven, it is linked to the asymmetry of the longitudinal component of the difference in velocities S:

$$C_1 = \frac{1{,}072}{\sqrt[3]{|S_1|}} . \tag{7}$$

Let us note that the constant C_1 can be determined experimentally only in the case when, along with the value of b, there is an independent determination of the energy dissipation ε. On the basis of some indirect data, A. N. Kolmogorov, in paper [3], gave the preliminary evaluation $C = 1.5$, which corresponds to $C_1 = 1.4$. If $S_1 = 0.4$ (as per Townsend), we derive $C_1 = 1.45$. This value practically coincides with the value of the constant C_1 as per Kolmogorov.

2. THE THEORETICAL EVALUATION OF THE STRUCTURAL CHARACTERISTICS OF THE FIELD OF THE WIND UNDER CONDITIONS OF THE LOWEST ATMOSPHERIC LAYER

As indicated above, the basic physical magnitude that determines the characteristics of the local structure of a turbulent current, is the dissipation of energy. In evaluating this magnitude in the lowest atmospheric layer, we will use the premise that the atmospheric layer up to the altitude of 10-15 meters can be treated, with some approximation, as a logarithmic boundary layer. For the purposes of the diagram of the logarithmic boundary layer, it is simple to obtain an expression for the transformation of the energy of the averaged current into the energy of turbulent pulsations. By disregarding the effect of the "diffusion" of the energy of turbulent pulsations in the conditions of the logarithmic boundary layer, we can assume, by virtue of the steadiness of the cycle, that the mean dissipation of energy of the turbulent pulsations at the given level coincides with the transformation of the energy of the averaged current into the energy of turbulent pulsations. (The validity of disregarding the effect of "diffusion of energy" of the turbulent pulsations may be substantiated with adequate rigidity by considerations of spontaneous congruency of the turbulent processes in the logarithmic boundary layer.) Based on these considerations, we derive the following expression for the value of the energy dissipation ε applying to a unit of mass:

$$\varepsilon = \frac{1}{\rho} \left(\tau \frac{d\overline{v}}{dz} \right), \tag{8}$$

where τ is the intensity of friction, $\overline{v}(z)$ is the distribution of the mean velocity of the current in height.

In the logarithmic boundary layer, τ = const. Let us introduce the velocity of friction v_*, assuming that

$$\rho v_*^2 = \tau,$$

and let us use what is known in the theory of the logarithmic boundary layer as the mean velocity $\bar{v}(z)$ expressed in terms of v_*, and the characteristic of the roughness of the underlying surface z_0:

$$\bar{v}(z) = \frac{v_*}{\chi} \ln \frac{z}{z_0}, \qquad (9)$$

where x = 0.4, is the Karman constant. It then follows from formula (8) on the basis of formula (9) that

$$\varepsilon = \frac{v_*^3}{\chi z}. \qquad (10)$$

To determine v_* and z_0, we must have reliable measurements of the mean velocity at several altitudes (at least two). After z_0 for the given conditions of a locality is determined v_* may be determined from one measurement of the mean velocity by using formula (9). For instance, when the roughness $z_0 = 1.2$ cm, $v_* = 0.083\, \bar{v}_{1.5}$, where $\bar{v}_{1.5}$ is the wind velocity at the altitude of 1.5 meters.

By using formula (10) and expression (5) for the internal scale of turbulence, an evaluation can be derived for the magnitude of this scale under the conditions of the lowest atmospheric layer. If we accept the value of asymmetry $S_1 = 0.4$, then, in the presence of a roughness $z_0 = 1.2$ cm and of a wind velocity $\bar{v}_{1.5} = 3.5$ m/sec for the altitude $z = 1.5$ m, we derive $\eta_1 \approx 0.5$ cm. The ratio

Declassified in Part - Sanitized Copy Approved for Release 2012/03/28 : CIA-RDP82-00039R000200060007-7

between the internal scale and altitude is only mildly pronounced -- the internal scale is in proportion to the 4th root of z, so that η_1 increases only twice in the transition from the altitude of 1.5m to the altitude of 24 meters.

The expression for the structural characteristic b can be obtained similarly by substituting the magnitude of ε from formula (10) into formula (6):

$$b = \frac{C_1 v_*}{\sqrt[3]{\chi z}} \tag{11}$$

and, consequently,

$$\frac{\sigma_{\Delta v}}{v_*} = C_1 \sqrt[3]{\frac{r}{\chi z}}, \tag{12}$$

where $\sigma_{\Delta v}$ is the mean quadratic transverse component of the difference of velocities at two points. This formula is valid when $\eta_1 \ll r \ll z$.

Let us take note that on the basis of considerations of the theory of congruence alone, the following "universal" ratio for the logarithmic boundary layer, valid in the presence of any $r \gg \eta_1$ comparable with z, is to be expected:

$$\frac{\sigma_{\Delta v}}{v_*} = f\left(\frac{r}{z}\right). \tag{13}$$

Formula (12) constitutes a particular case of formula (13). If in formula (12), V_* is expressed in terms of the value of the mean velocity, we derive the following expression for the ratio between the mean quadratic difference of velocities and the mean velocity at the given altitude:

$$\frac{\sigma_{\Delta V}}{V} = C_1 \sqrt[3]{\frac{r}{\varkappa z}} \frac{1}{5.7 \log z/z_0} \qquad (14)$$

or

$$\frac{b}{V} = \frac{C_1}{\sqrt[3]{\varkappa z} \; 5.7 \log \frac{z}{z_0}} \qquad (14,a)$$

Experimental research into the microstructure of the field of the wind under the conditions of the lowest atmospheric layer is concerned not only with the checking of the applicability of the "two thirds law" to atmospheric turbulence and with the determination of the values of the structural characteristic b, but also with the comparison of the experimentally derived values of b with their theoretical evaluation as per formula (14). To accomplish this we must have sufficiently reliable measurements for the distribution of mean velocity with altitude in addition to the measurements of turbulent pulsations.

3. THE METHODS FOR THE MEASUREMENT OF TURBULENT PULSATIONS

For the study of turbulence in wind tunnels, the thermoanemometric method which at the present time is practically the only method for the measurement of rapid pulsations of current velocity is widely used. A thermoanemometer was therefore used in the study of the microstructure of the wind. (The first attempt in this direction was undertaken by the author together with N. D. Yershova in 1941 [12]. In reference to the problem of using the thermoanemometer for the study of atmospheric turbulence, see also [10].)

The action of the thermoanemometer is based on the use of the ratio between the temperature of a fine metal thread, heated by an electric current, and the velocity of the air current [11]. The detailed description of the thermoanemometric method for the measuring of the velocity of the current and of the turbulent pulsations, is beyond the framework of this work. We will limit ourselves to a short description of the differential thermoanemometer, designed at the Geophysical Institute of the Academy of Sciences USSR for the special purpose of studying atmospheric turbulence. (The experimental part of this work was done together with S. I. Krechner.)

The receiving part of the device, the thermo-fitting, is a fine platinum wire, 20 microns in diameter, stretched in a special holder (see Figure 1). In operation the wire which is arranged vertically is heated by an electric current of about 0.2 - 0.25 ampere and the holder fork is oriented into the wind in order to reduce aerodynamic resistance to a minimum.

In measuring the differences of the momentary values of current velocity, a Wheatstone bridge is wired into the two points of the thermo-fitting. We made use of a special wiring diagram (combination bridge), which makes possible the simultaneous determination changes in the resistance of the fittings [at the two points], as well as the sum of their resistance (see Figure 2). Such a wiring diagram for the thermo-fittings provides for the simultaneous registration of both the difference in the velocities, as well as of the mean velocity at the points of mensuration. (The momentary values for the mean velocity of the current must be known in order to determine the sensitivity of the galvanometer Γ_1 to the difference in the velocities, since this coefficient depends substantially on the velocity of the current, as a result of the non-linearity of the characteristics of the thermo-fitting.)

Figure 1. The thermo-fitting.

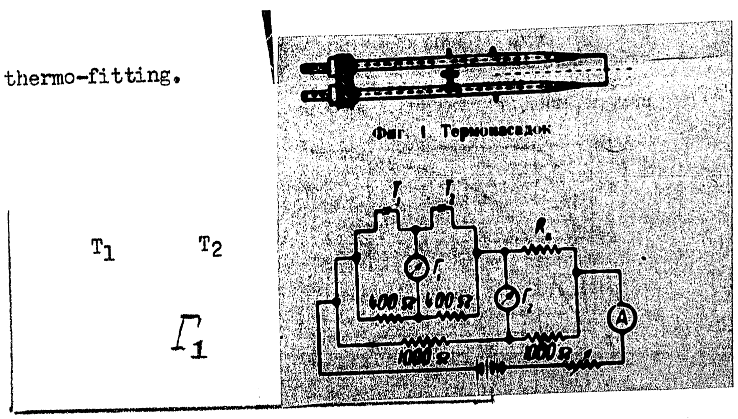

Figure 2. Wiring diagram of the Wheatstone bridge connection to the thermoanemometer: T_1 and T_2 — thermo-fittings; galvanometer Γ_1 reacts to the difference in the resistances; galvanometer Γ_2 — reacts to the sum of resistances.

In our experiment we used as registering galvanometers the loops of a 10-loop oscillograph of Geophysical Institute design, with a sensitivity of 5×10^{-6} amperes/millimeters, in the presence of an inherent frequency of 130 cycles. The "static characteristics" of the thermo-fittings were obtained by means of a corresponding calibration of the installation in a wind tunnel. Figure 3 is an example of a thermo-fitting calibration curve. Since the results of thermo-fitting calibrations may show some variation correction potentiometers were introduced into the wiring network of the Wheatstone bridge (these are not shown in Figure 2 above). These correction potentiometers provide for the electrical equalization of the sensitivity of the thermo-fittings. With the proper mounting of these potentiometers, galvanometer Γ_1 remains at zero reading, when thermo-fittings mounted very close to each other, are subjected to a current of changeable velocity. Figure 3 also depicts the sensitivity curve K of the device to the difference of the velocities. This curve is derived by graphic differentiation of the thermo-fitting calibration curve with its subsequent translation into terms of the sensitivity of galvanometer Γ_1 to the small variations of resistance in the thermo-fitting circuit. Due to the considerable overheating of the thermo-fittings with relation to the surrounding environment, the effect of the air temperature upon the calibration curve is, generally speaking, negligible. However, in making the measurements under natural conditions, we were introducing corrections for the mean air temperature. The methods of interpolating these corrections were worked out by S. I. Krechmer.

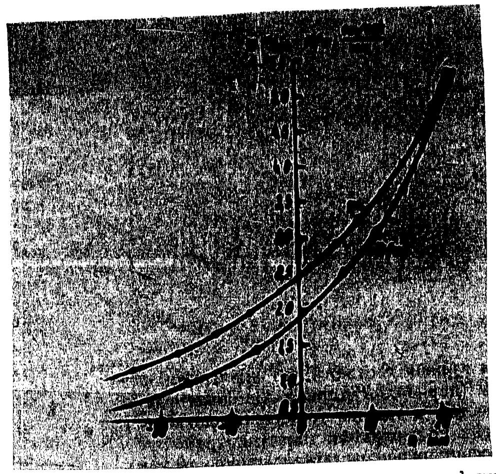

Figure 3. Thermo-fitting calibration curve — curve showing sensitivity to the difference in velocities.

In addition to deriving the calibration curves (for static characteristics) of the instrument, we also obtained the "dynamic characteristics" of the instrument — the behavior curve under a sudden change in operating conditions of the thermo-fitting. As was demonstrated by S. I. Krechmer [13], the resistance curve for the wire, as a function of an abrupt change in the velocity of the air current which must be known in order to determine the time constant coincides with a similar behavior curve for a sudden change in the heating current with a constant velocity of the air flow. The derivation of the latter curve may be effected with the aid of an oscillograph, with sufficiently rapid rectification provided. This method was used for the derivation of calibration curves for the entire apparatus. Figure 4 depicts such a calibration curve for a thermoanemometric apparatus. A calibration curve for one galvanometer is depicted in the same graph. A comparative study of the two curves reveals that the inertia of the apparatus is basically determined by the thermal inertia of the thermo-fitting, and to a lesser degree by the inertia of the galvanometer. The knowledge of the dynamic characteristics of the thermoanemometer made the evaluation of the time constant of the device possible -- it is about 10-15 milliseconds. As will be subsequently seen, a direct determination of the time constant of the thermoanemometer is very essential for the correct interpretation of the experimental results obtained.

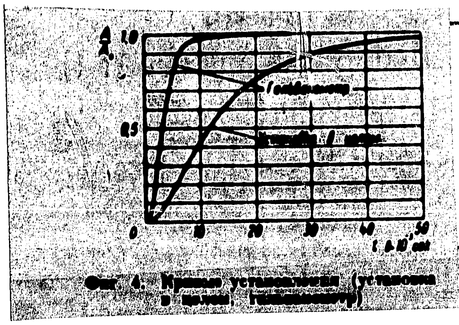

Galvanometer

Apparatus as a whole

t in 10^{-3} sec

<u>Figure 4</u>. Determination curves (for the entire apparatus; for the galvanometer).

In investigating the structure of turbulence in the lowest atmospheric layer, we used the following arrangement. The thermo-fittings were mounted in a special extension-type carrier (see Figure 5), allowing for their placing at various distances from each other, within a range of 0.5-60 centimeters. The carrier was equipped with a weather vane, for the purpose of setting the thermo-fittings against the wind, and with a special stop to keep the carrier in place, while measurements are being taken. The entire system permitted remote control and was connected by cable to an appropriate electrical circuit and to an oscillograph. When investigating the structure of atmospheric turbulence at various altitudes, the carrier was mounted on a theodolite tripod (1.5 meters high) or on a telescopic mast, which permitted the raising of the carrier to an altitude of from 3 to 15 meters. In addition to the thermo-fittings, a Fuss cup anemometer, equipped with a special electromagnetic transmitting element, providing for the recording of the anemometer revolutions upon the oscillograph tape was mounted on the above carrier. Similar anemometers were mounted on poles at various altitudes so that it was possible to derive the distribution of the mean wind velocity in the lowest atmospheric layer up to 15 meters.

Figure 5. Extension-type carrier for mounting the thermo-fittings. (See Appendix)

Figure 6 shows a sample of an oscillogram ($\frac{1}{2}$ scale), obtained during the investigation of the wind microstructure in 1948 at an altitude of 3 meters above the soil. The upper curve corresponds to the values of the difference in the velocities of the current on a base of 8 centimeters (base perpendicular to the direction of the wind); the lower curve corresponds to the sum of the velocities at the same points (non-linear scale). The oscillogram is divided vertically into time divisions representing intervals of 1/7 of a second. The readings of the four Fuss anemometers, equipped with electromagnetic transmitting elements, are recorded at the bottom of the oscillogram, each ejection of a definite mark corresponds to one revolution of the anemometer.

Figure 6. Specimen of differential thermoanemometer recording (difference of velocities on a base of 8 centimeters). (See Appendix)

For an empirical determination of the structural function, the carrier was mounted at predetermined levels (1.5; 3; 15 meters), and the readings of the thermoanemometer were recorded by oscillograph at various distances between the thermo-fittings. The measurements were made for 15-20 seconds at each base, beginning with the small bases, followed by a gradual extension of the carrier terminals to a spacing of 60 centimeters, after which repeat observations were made in reverse order with the gradual diminution of the bases. (While readings and measurements are being taken the entire system is at rest.) Figure 7 shows sections of recordings corresponding to a distance between the thermo-fittings of 2, 4, and 8 centimeters. A comparative study of these recordings visually reveals the manner in which the range of the difference in the wind velocities at two points of the current is increased, with an increase in the base. A very meticulous processing of the oscillograms yields the quantitative characteristics of the turbulent pulsations, and, particularly, permits the construction of the empirical structural functions.

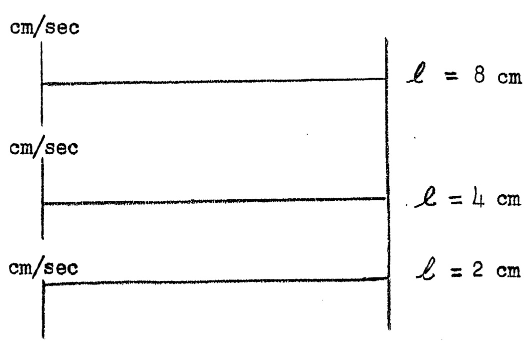

Figure 6. Specimen of differential thermoanemometer recording (difference of velocities on a base of 8 centimeters). (see Appendix)

For an empirical determination of the structural function, the carrier was mounted at predetermined levels (1.5; 3; 15 meters), and the readings of the thermoanemometer were recorded by oscillograph at various distances between the thermo-fittings. The measurements were made for 15-20 seconds at each base, beginning with the small bases, followed by a gradual extension of the carrier terminals to a spacing of 60 centimeters, after which repeat observations were made in reverse order with the gradual diminution of the bases. (While readings and measurements are being taken the entire system is at rest.) Figure 7 shows sections of recordings corresponding to a distance between the thermo-fittings of 2, 4, and 8 centimeters. A comparative study of these recordings visually reveals the manner in which the range of the difference in the wind velocities at two points of the current is increased, with an increase in the base. A very meticulous processing of the oscillograms yields the quantitative characteristics of the turbulent pulsations, and, particularly, permits the construction of the empirical structural functions.

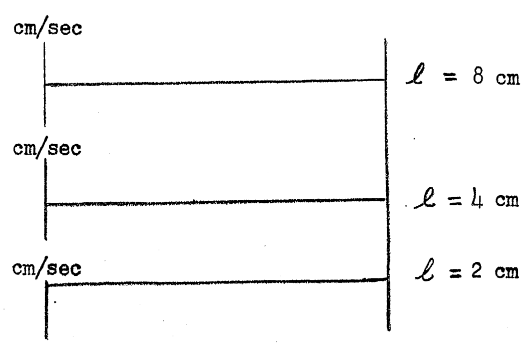

Figure 7. The difference in the wind velocities at the distances of 2, 4, 8 centimeters.

This paper is concerned with the results of measuring the characteristics of the turbulence structure in the lowest atmospheric layer. Using the same methods the author, together with N. Z. Pinus and S. I. Krechmer, made an attempt to obtain microturbulence data on the free atmosphere during a free-balloon flight. The results of this expedition are given in a separate article [14].

4. THE EFFECT OF THE INERTIA OF THE APPARATUS UPON THE EMPIRICALLY DETERMINABLE STRUCTURAL FUNCTION OF THE FLOW

Before we embark upon a detailed discussion of the results of measuring turbulence by means of the above described apparatus, we must ascertain the degree to which the inertia of the apparatus involved will affect the results of the measurement of the structural function of the flow. In using the thermoanemometer for the measurement of the turbulent pulsations of the flow velocity in wind tunnels, the effect of the inertia of the device is quite substantial. To eliminate this effect, special compensating loops are introduced into the wiring of the booster, which is connected to the thermo-fitting [11]. In measuring turbulent pulsations in the atmosphere we did not use a booster or any other compensating device. In such cases it becomes necessary to keep a special check on the distortions generated during the determination of the structural function of the flow by means of measuring the pulsations by a device whose time constant is considered known. The inertia of an apparatus can be characterized by the "time constant" of the apparatus M, assuming that

$$\frac{du}{dt} = \frac{1}{M} \left(v(t) - u(t)\right), \tag{15}$$

where u(t) is some conditional velocity of the flow, computed by the readings of the thermoanemometer on the basis of its static characteristic $v(t)$ is the true velocity of the flow. Magnitude M as a rule depends on the velocity of the flow, yet within the limits of a single reading it may be considered as a constant corresponding to the mean velocity of the current $\overline{v}$ during the measuring time interval. As was indicated above, the magnitude of the time constant M can be determined empirically. In the case of our installation, with $\overline{v} = 3$ m/sec, $M \approx 0.015$ sec.

(Equation (15) corresponds to the exponential curve of cycle determination. In the case where the inertia of the installation is governed not only by the thermal inertia of the thermo-fitting, but also by the mechanical inertia of the recording galvanometer, equation (15) should have been replaced by some more complex equation of the third order. However, when dealing with an sufficiently rigid galvanometer, it is acceptable, for the purpose of practical computations, to approximate the determination curve by using the exponential curve, and to use equation (15), assuming that M summarily characterizes the thermal inertia of the thermoanemometer and the inertia of the galvanometric system.)

By integrating equation (15), we derive the law of averaging of the momentary velocities in time, conforming to an apparatus of a given inertia M:

$$u(t) = \frac{1}{M} \int_0^\infty e^{-\frac{\tau}{M}} v(t-\tau)\, d\tau \qquad (16)$$

Practically, of course, the upper limit of the integral (16), due to the rapid decrease of the function under the integral sign, may be replaced by a value on the order of magnitude of several M's. The averaging in time may be replaced by averaging in space along the flow, on the assumption that the vortices defining the velocity pulsations of the flow are transferred by the flow itself at a velocity close to $\bar{V}$. By introducing a new variable $\xi = v\tau$, we derive

$$u(t) = \frac{1}{\lambda} \int_0^\infty e^{-\xi/\lambda} v(t, \xi)\, d\xi, \qquad (17)$$

where

$$\lambda = M\bar{v} \qquad (18)$$

the "averaging scale" of the apparatus, is in conformity with the mean velocity of the flow, and ξ is the coordinate measured from the apparatus in the direction of the flow. The "averaging scale" λ, in the case of a flow velocity of 3 m/sec for our installation, is about 5 centimeters. In addition to the averaging of the field of pulsation along the flow induced by the inertia of the apparatus, there is also an averaging in a transverse direction, along the thread of the thermo-fitting. However, with a thread length of 2 centimeters the basic part is played by the longitudinal averaging, so that in subsequent computations we will reckon with the latter factor only. Knowing the law of averages for the field of pulsations, and having hypothetically assumed a definite form of the theoretical structural function, we can now compute the ratio between the readings of the differential thermoanemometer having a predetermined inertia (the value of the "averaging scale" λ), and the distance between the points of mensuration. In this paragraph we will conditionally call this ratio the "empirical structural function". Comparison of such a computation with the data derived by measurements from direct readings of the apparatus provides for a check on the hypothetical structural function, and together with this, for the determination of the parameters of this function on the basis of experimental data, with allowance for the inertia of the measuring apparatus.

We select for the analysis of the theoretical structural function the two thirds law:

$$D_{nn}(r) = b^2 r^{2/3}, \qquad (19)$$

$$D_{ll} = \tfrac{3}{4} b^2 r^{2/3} \qquad (20)$$

We remenber that the thermo-fitting perceives the projection of the pulsation velocity upon the direction of the flow. For further computations, it will be necessary to have the formula for the mean square of the difference of the above indicated projections of the pulsation velocity at the ends of the segment, forming with the mean direction of the flow the angle φ :

$$D_{\varphi}(r) = D_{nn}(r) \sin^2\varphi + D_{ll}(r) \cos \varphi = \qquad (21)$$

$$= D_{nn}(r) + (D_{ll} - D_{nn}) \cos^2\varphi = b^2 r^{2/3} (1 - \tfrac{1}{4} \cos^2 \varphi).$$

Let us take the direction of the x-axis in the direction of the flow, the y-axis in the direction of the measurement base (perpendicular to the direction of the flow). Let us designate the momentary value of the instrumental reading at point M_1 by u_1, the same at point M_2 by u_2, and the value of the pulsation velocity component in the direction of the x-axis by v. Then, on the basis of formula (17), the difference in the instrument readings, taken at points M_1 and M_2, can be presented in the following form:

$$u_2 - u_1 = \frac{1}{\lambda} \int_0^{\infty} e^{-x/\lambda} \left[v(x, l) - v(x, 0) \right] dx.$$

Let us raise both parts of the above formula to the power of 2 and average them (statistically):

$$\overline{(u_2-u_1)^2} = \frac{1}{\lambda^2}\int_0^\infty\int_0^\infty e^{-x/\lambda}e^{-x'/\lambda}\,[\overline{(v(x,l)- \qquad (22)$$

$$\overline{-v(x,0))(v(x',l)-v(x',0))}]\,dx\,dx'$$

The necessity for the computation of similar integrals occurs in some problems dealing with atmospheric acoustics [4]. In the case of an isotropic or local-isotropic flow the correlation moment of the differences of the velocities, which is under the integral sign in formula (22), is easily expressed in terms of the structural function of the flow:

$$\overline{(v(x,l)-v(x,0))(v(x',l)-v(x',0))} =$$

$$= \frac{1}{2}[\overline{(v(x,l)-v(x',0))^2} + \overline{(v(x,0)-v(x',l))^2} -$$

$$- \overline{(v(x,l)-v(x',l))^2} - \overline{(v(x,0)-v(x',0))^2} = \qquad (23)$$

$$= D_\varphi(r) - D_{ll}(|x-x'|),$$

where

$$r^2 = l^2 + (x'-x)^2, \quad \cos^2\varphi = \frac{(x'-x)^2}{r^2}$$

Now, by substituting expressions (20), (21) for D_{ll} and D_{φ} in formula (23), we can express $\overline{(u_2 - u_1)^2}$ in the following form:

$$\overline{(u_2-u_1)^2} = \frac{b^2}{\lambda^2} \int_0^\infty \int_0^\infty e^{-\frac{x'+x}{\lambda}} \left\{ \left[(x'-x)^2 + l^2 \right]^{1/3} \left(1 - \frac{1}{4} \frac{(x'-x)^2}{l^2+(x'-x)^2} \right) - \frac{3}{4} |x-x'|^{2/3} \right\} dx\, dx' \tag{24}$$

By introducing the new variables $\frac{x'+x}{\lambda}$ and $\frac{x'-x}{\lambda}$ we succeed in performing one integration and after simple transformations we derive the final result in the following form:

$$\overline{(u_2-u_1)^2} = b^2 \lambda^{2/3} f(l/\lambda), \tag{25}$$

where the function $f(\eta)$, with $\eta = \frac{l}{\lambda}$, is given in the integral into which η enters as a parameter:

$$f(\eta) = \int_0^\infty e^{-v} \left\{ (v^2+\eta^2)^{1/3} \left(1 - \frac{1}{4} \frac{v^2}{v^2+\eta^2} \right) - \frac{3}{4} v^{2/3} \right\} dv. \tag{26}$$

The values of integral (26) determining $f(\eta)$, were computed by the method of numerical integration by A. M. Yaglom and A. V. Perepelkina, and are cited in Table 1 below, from η 0.1 to 20.

TABLE 1

The values of function $f(\eta)$

η	0.01	0.05	0.1	0.2	0.3	0.4	0.5	1	1.5	2
$f(\eta)$	0.001	0.008	0.022	0.059	0.108	0.157	0.215	0.480	0.739	0.987
η	4	6	8	10	12	14	16	18	20	
$f(\eta)$	1.873	2.643	3,334	3,975	4,571	5,137	5,677	6,195	6,694	

With high values of η (the base being much greater than the averaging scale), the following asymptotic representation takes place:

$$f(\eta) \approx \eta^{2/3} - \frac{3}{4}\Gamma\left(1+\frac{2}{3}\right) + \frac{1}{6}\eta^{-4/3}.$$

When $\eta \geqslant 8$, it is permissible to be limited to the first two terms, with the error not in excess of 1 percent. Thus, in the case of a base which is considerably greater than the scale of averaging λ, we have

Declassified in Part - Sanitized Copy Approved for Release 2012/03/28 : CIA-RDP82-00039R000200060007-7

$$\overline{(u_2 - u_1)^2} = b^2 l^{2/3} - 0.677 b^2 \lambda^{2/3}. \tag{27}$$

In our measurements the value of l was changing within the limits from 2 to 60 centimeters, which, with $\lambda = 4 cm$, corresponds to a range in the change of η from 0.5 to 15. In order to apply the above quoted computations to the processing of experimental data, it is advisable to give a simpler representation (with an approximation of about 1 to 2 percent) of function $f(\eta)$ within the working range of η. It turned out that if which corresponds to the mean quadratic difference of the velocities is laid off along the ordinate, and $\sqrt[3]{\eta}$ is laid off along the abscissa, then, within the range of variation of η from 0.5 to 15, the corresponding curve may be replaced by a straight line with a considerable degree of precision (see Figure 8).

$\sqrt{f(\eta)}$

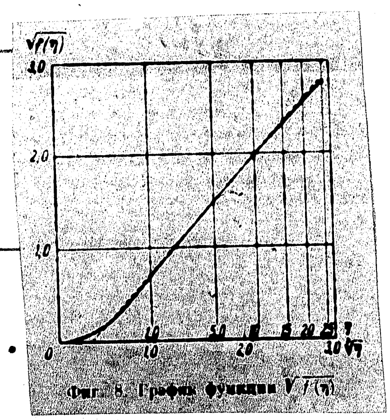

Figure 8. Graph of function $\sqrt{f(\eta)}$.

By using the equation of this straight line for the range of variation of η with which we are concerned we derive the following working formula:

$$\sqrt{f(\eta)} = 1.11\left(\sqrt[3]{\eta} - 0.37\right),$$

and correspondingly with this:

$$\sigma_{\Delta u} = \sqrt{\overline{(u_1 - u_2)^2}} = 1.11\, b\left(\sqrt[3]{\mathcal{l}} - 0.37\sqrt[3]{\lambda}\right). \quad (28)$$

The above computation indicates that the experimental data on the structural function obtained in our measurements can be conveniently processed by laying off the value of the cube root of the base $\mathcal{l}$ along the abscissa, and the corresponding mean quadratic values of the difference between the velocities at two points along the ordinate. If the two thirds law is valid, the respective experimental points are to be on a line whose angular coefficient differs only by the constant factor 1.11 from the value of the structural characteristic of the flow. In this case the straight line is to intersect the abscissa to the right of zero, at a point corresponding to $\sqrt[3]{\mathcal{l}} = 0.37\sqrt[3]{\lambda}$. It must be noted that in evaluating the matching of the experimental data with the theoretical law for the structural function, the possibility of an independent evaluation of the displacement of the experimental straight line with relation to the origin of the coordinates, on the basis of the inertia data of the apparatus, is very essential. In the absence of such an independent evaluation the probability of a random "adaptation" of the experimental data to fit the theoretical formula (28) with the exponent 1/3, would be considerably increased.

5. THE RESULTS OF THE EXPERIMENTAL DETERMINATION OF THE STRUCTURAL FUNCTION IN THE LOWEST ATMOSPHERIC LAYER

This paper utilizes the results of the measurements of turbulence pulsations made in September 1948 near Moscow. The observational data obtained over a 3 day period was processed. The apparatus employed was described above in paragraph 3. Measurements were conducted over an adequately exposed observation stage. The pattern of the mean wind velocities was determined with the aid of Fuss anemometers, equipped with remote control transmitting elements (at 0.5-, 1-, 2- and 15-meter altitudes). The differences in the velocities were recorded on bases of 2, 4, 8, 16, 32, and 60 centimeters. Measurements using these bases were conducted at the altitudes of 1.5, 3, and 15 meters.

Following the primary processing of the oscillograms (the reading off of the ordinates at intervals of 1/7 of a second, the translation of the ordinates into terms of the difference in velocities), the mean absolute values of the difference in velocities over the recording period were computed.

(The location of the beginning of the count (the zero line) for the curve showing the difference in velocities was determined empirically as the mean value of the ordinate of the difference in velocities over the time of observation. The replacement of the mean quadratic departures by the mean absolute departures causes no essential change, except that it considerably simplifies the processing of the empirical data.)

With the selected recording time for each base, the number of processed points for each category was 40-60. The apparatus employed did not provide for the synchronous recording of the difference in the velocities, in the presence of different magnitudes of the base. The recordings for different bases thus referred to different conditions in the atmosphere. The mean velocity was changing particularly in passing from one recording to the next. In order to obtain comparable data we used the ratios of the mean absolute difference of the velocities to the mean wind velocity for the recording period, relying in so doing upon the general considerations of the theory of congruence. (Wind velocity in this case was taken by the thermoanemometer so as to reduce the chance of an error induced by the divergence in the scales of various devices.) Practically, the value of the "mean relative range", conforming to each value of the base and altitude of observation, was determined from the graph ($\overline{V}, \overline{\Delta V}$) constructed with the aggregate of the empirical data for the given conditions (base, altitude). Such a graph is shown in Figure 9. The angular coefficient k corresponding to the straight line $|\overline{\Delta V}| = k\overline{V}$ and to the mean relative range of the difference of velocities, was determined by the method of least squares.

$|\overline{\Delta V}|$ cm/sec

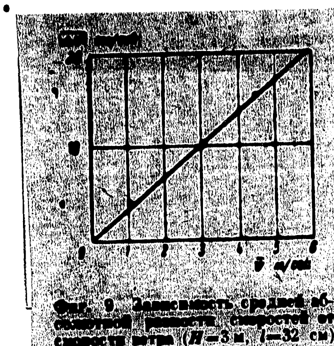

$\overline{V}$ m/sec.

Figure 9. Ratio between the mean absolute difference of velocities and absolute difference of velocities and wind velocity (H = 3m, ℓ = 32 cm).

The values of the mean ratios $\dfrac{\overline{|\Delta V|}}{\overline{V}}$ (in percent), which were determined by this method on the basis of all the data available for the various values of the base ℓ and altitude H, are listed in Table 2, with the number of recordings, by means of which the values given in parentheses were determined. The results obtained are shown graphically in Figure 10.

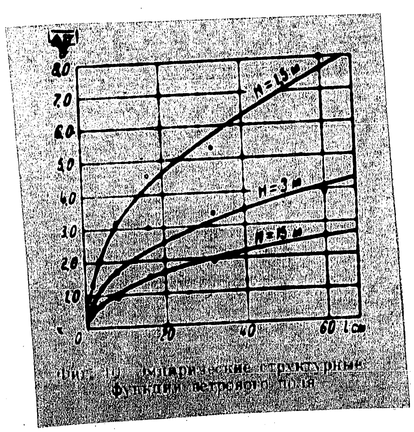

TABLE 2

Mean absolute differences of velocity in percent of the mean velocity

H, in m	ℓ, cm					
	2	4	8	16	32	60
1.5	1.3 (4)	2.1 (4)	3.2 (4)	4.6 (3)	5.4 (3)	8.0 (4)
3	0.7 (3)	1.2 (3)	1.7 (4)	3.0 (2)	3.4 (3)	3.9 (3)
15	0.5 (3)	0.7 (3)	0.9 (2)	1.5 (2)	1.9 (2)	2.6 (2)

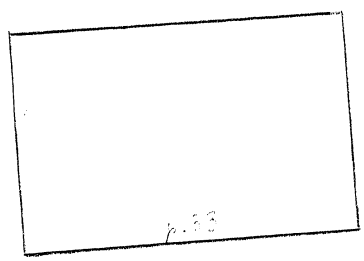

Figure 10. The empirically derived structural functions of the field of the wind.

It follows from Table 2 that, with the base fixed, the relative value of the difference in velocities is considerably reduced with an increase in altitude, as was to be expected on the basis of theoretical considerations. Using the recordings of the difference in velocities of sufficient duration (about 20 seconds), we determined the conversion factor for the determination of the mean quadratic values of $\sigma_{\Delta V}$ by the mean absolute values of $|\overline{\Delta V}|$. On the basis of statistical studies of three recordings the following formula for the computation of $\sigma_{\Delta V}$ was accepted:

$$\sigma_{\Delta V} = 1.29\,|\overline{\Delta V}|. \tag{29}$$

Let us take note of the fact that the factor 1.29 is very close to the 1.25 value, which is in conformity with the Gauss law.

The empirical data, cited in Table 2, can be used for comparison with the theoretical structural function law and for the determination of the values of the structural characteristic b (it is more convenient to determine the ratio of b to the velocity of the current). Figure 11 shows the ratio between the empirical values $\frac{|\overline{\Delta V}|}{V}$ and $\sqrt[3]{\ell}$ (ℓ is the base) for three altitudes. The straight lines are plotted by the method of least squares. All straight lines intersect the abscissa to the right of the origin of coordinates. The respective values of the abscissas for the intersection point for the three graphs corresponding to altitudes 1.5, 3, and 15 meters are close to each other and conform to

$\sqrt[3]{\ell_1} = 0.63$. If the displacement of the graphs in Figure 11 is interpreted as a result of the inertia of the apparatus (in conformity with the deductions of the preceding paragraph), we can, in conformity with formula (28), put down for the above derived value $\sqrt[3]{\ell_1} = 0.63$ the corresponding "average scale" $\lambda \approx 5$ cm. This value is in complete agreement with the average scale of directly determined by means of investigating the inertia of the apparatus in the wind tunnel test (by the calibration curve). Thus, we can maintain with adequate assurance that the results of our measurements demonstrate the applicability of the "two thirds law" to turbulence in the lowest atmospheric layer.

(The decisive factor for such an assumption is the agreement between the displacement of the empirical structural curve with the independently measured inertia of the apparatus. For check purposes we constructed the graphs $\left(\frac{|\Delta V|}{V}, \ell^{\alpha}\right)$ with exponents $\alpha = 1/2$ and $\alpha = 1/4$. Although with these exponents the experimental points are almost perfectly on the lines, the displacement of the resulting straight lines with relation to the origin of the coordinates, is in sharp disagreement with the data on the inertia of the apparatus (in the first case, displacement is completely absent, in the second case, it is twice the computed value).

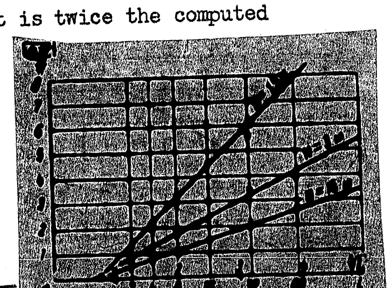

Figure 11. Ratio between $\frac{|\Delta V|}{V}$ and $\sqrt[3]{\ell}$ as per the empirical data.

Below are given the values $b/\sqrt{\ }$ (b is the structural coefficient in formula (28)), which were determined by the experimental curves (see Figure 11). These values are obtained by multiplying the angular coefficient of the corresponding curve by 1.29 (for the conversion of the mean absolute differences into mean quadratic differences), and by dividing the correction factor 1.11 (see preceding paragraph).

It is of interest to juxtapose the characteristics of the microstructure of the wind obtained by direct measurements with the distribution of the mean wind velocities. Figure 12 is a graph depicting the distributions of mean velocities for four series of observations (the scale along the z-axis is logarithmic). All four cases are in satisfactory agreement with the logarithmic law of velocities which permitted the determination of the "roughness" value $z_0 = 1.1$ cm.

TABLE 3

H, m	1.5	3	15
$b/\sqrt{\ }$, $cm^{-1/3}$	0.029	0.015	0.010

Fig 12. Mean Velocity Distributions by height

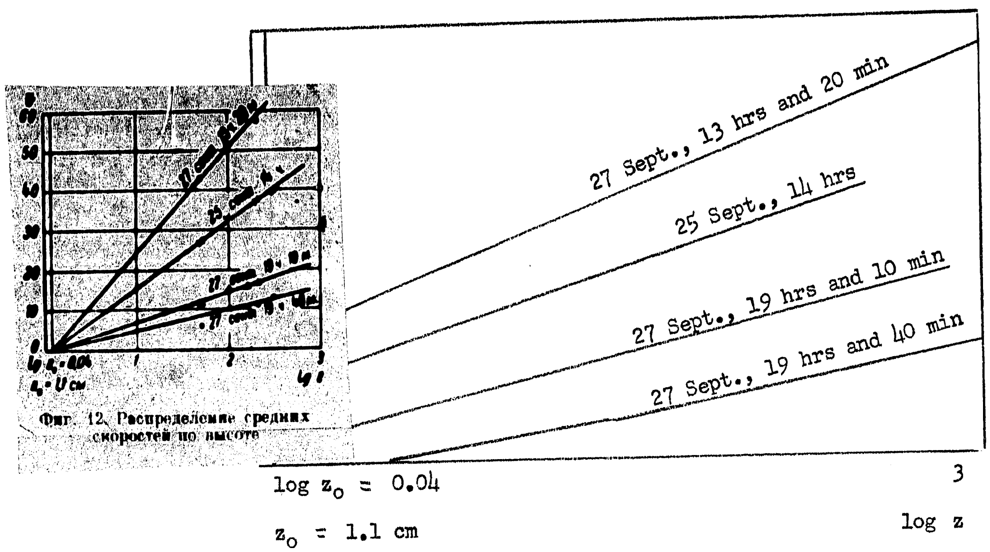

In paragraph 2, a theoretical evaluation (14) was given for the ratio between the structural characteristic b and the mean wind velocity in the conditions of the logarithmic boundary layer:

$$\frac{b}{V} = C_1 F(z), \qquad (30)$$

where

$$F(z) = \frac{1}{\sqrt[3]{\chi z}\; 5.7 \log \frac{z}{z_0}}$$

C_1 is an arbitrary constant approximately equal to unity, $\chi = 0.4$ is the Karman constant.

Using the above derived value of roughness $z_0 = 1.1$ cm, we computed the values $F(z)$ for observation altitudes of 1.5, 3, and 15 meters, and compared these values with the actually observed values $b/\bar{V}$ (see Figure 13), for the purpose of evaluating the arbitrary constant C_1, the only numerical constant entering into the computation formulas. On the basis of our measurements

$$C_1 \approx 1.1$$

A certain scattering of the points in Figure 13 is fully understandable, since the theoretical computation of energy dissipation on the basis of the hypothetical logarithmic layer, in its application to the varying conditions in the real atmosphere, is only a rough evaluation. The value of the constant $C_1 \approx 1.1$ is somewhat less than 1.4, which value conforms with the Townsend and Dryden [3, 9] observations. It should be kept in mind that the absolute value of C_1 may contain a certain error due to the disparity between the scales of the thermoanemometer and the Fuss anemometers, an error due to the determination of $|\overline{\Delta V}|$ using a relatively short time interval, an error in the conversion factor from $|\overline{\Delta V}|$ to $\sigma_{\Delta V}$, etc. However, the total relative error in the determination of C_1 in our measurements could hardly have been in excess of 20 percent.

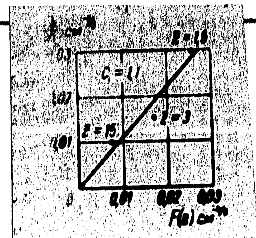

Фиг. 13

Figure 13

6. MEASUREMENT OF THE VERTICAL COMPONENT OF WIND VELOCITY AND DETERMINATION OF TURBULENT FRICTION

The apparatus we used in investigating the microstructure of the wind was also used by us for the measurement of the vertical component of wind velocity. On the basis of these recordings a determination was made in several cases of the turbulent friction (the Reynolds stress) in the lowest atmospheric layer.

In gauging the vertical component of velocity, a transmitting element of special design -- an "angular thermo-fitting", was connected with the above described electrical network (a combination Wheatstone bridge with recording on a loop oscillograph designed by the Geophysical Institute, Academy of Sciences USSR). The design of the angular thermo-fitting is shown in Figure 14. The receptors are two platinum threads (30 microns in diameter), arranged at an angle of 45 degrees to the axis of the fitting, and the connections playing the part of the arms of the bridge. In operation the plane of the fitting is arranged vertically so that its axis is in a horizontal plane. The fitting is pointed into the wind by means of a special weather vane (see Figure 15). When the flow is strictly horizontal both threads of the thermo-fitting are under the same cooling conditions. The bridge in this case is balanced at zero. When the flow velocity vector is inclined with relation to the axis of the fitting, the conditions of cooling are different for the upper and lower thread, and as a result an electric current is generated in the diagonal of the bridge which depends on the angle of inclination of the velocity vector. This ratio, within the limits of $\pm$ 15 degrees, is practically linear. The corresponding factor of proportionality is a function of the velocity of the flow. The velocity of the flow is determined by the sum of resistance (see the structure of the bridge, paragraph 3), by means of a calibration curve.

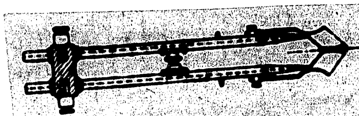

Фиг. 14. Угловой термонасадок

Figure 14. Angular thermo-fitting.

Figure 15. Weather vane for the angular thermo-fitting. (2a 34)

For calibrating the angular thermo-fitting is placed in the wind tunnel on a special holder by means of which the angle between the axis of the fitting and the direction of the current in the wind tunnel may be varied as desired, this operation being repeated at various flow velocities.

The above described method of measuring the vertical wind component was used in the experiments by A. P. Constantinov [15]. However, the thermo-fitting of our design has a lower inertia together with a higher sensitivity of the entire apparatus. The inertia of our apparatus is approximately 0.02 seconds, which makes it possible, in the solution of a number of meteorological problems, to consider it as practically inertia-free.

When operating with an angular thermo-fitting, the oscillogram shows two curves (see Figure 16), of which the lower one corresponds to the change in the velocity of the current (velocity vector modulus), and the upper one corresponds to the vertical component (the angle of inclination). In processing the recordings obtained with the angular thermo-fitting the velocity of the flow is determined first, after which the sensitivity to the change in the angle of inclination for the given velocity is determined. In practical processing we used a special nomogram in order to generalize the results of the calibration of the thermo-fitting in the wind tunnel for various velocities and various angles of inclination. The observed values of the vertical component of wind velocity, as a rule, do not exceed 10 percent of the mean flow velocity. This corresponds to angles of inclination of ± 6 degrees. Figure 17 shows the distribution curve for the angles of inclination of the wind at an altitude of 1.5 meters.

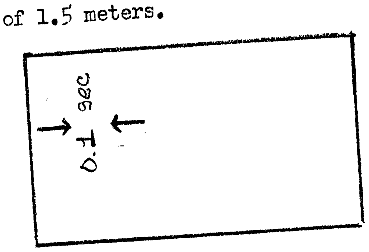

Figure 16. Specimen of the recording of the vertical component of wind velocity.

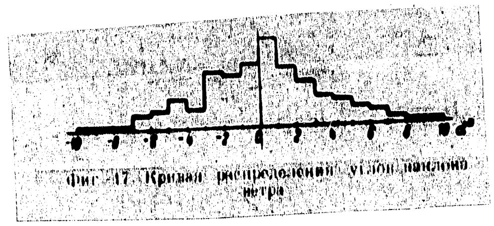

Figure 17. Distribution curve of the angles of inclination of the wind.

With the accumulation of the synchronous recordings of the momentary values of the vertical and horizontal wind velocity components over an adequately long period of time it becomes possible to compute the intensity of turbulent friction τ by using the direct determination of this quantity by Reynolds [16]

$$\tau = -\overline{\rho u' w'} \tag{31}$$

where ρ is the density of the environment, u' and w' are the pulsations of the horizontal and vertical wind velocity components. For the characteristic of friction the dynamic velocity V_* determined in terms of τ, is frequently used:

$$V_*^2 = \frac{\tau}{\rho}. \tag{32}$$

Figure 18 is a correlation graph of the momentary values of u' and w', plotted on the basis of a 20-second recording (the points were plotted at 0.1 second intervals). As was to be expected, u' and w' manifest a perceptible negative correlation (R = -0.65). The dynamic velocity computed with this data turned out to be

$$V_* = 0.33 \text{ m/sec.}$$

Let us note that the indirect method frequently used in meteorology for the computation of friction by the distribution of the mean wind velocities,

$$V_{*} = \varkappa z \frac{du}{dz} \qquad (33)$$

in this case, results in $V_{*} = 0.45$ (it is assumed that $\varkappa = 0.4$. For a single observation the divergence is not very great.

Thus, inertia-free measurements of the wind velocity pulsations (of the longitudinal and vertical component) open up the possibility for the direct determination of turbulent friction in the lowest atmospheric layer. The "absolute" measurements of turbulent friction are of primary importance to the physics of the lowest atmospheric layer as a check upon the indirect methods of computing the characteristics of atmospheric turbulence which at the present time are widely used in meteorology [17].

Academy of Sciences USSR,
Geophysical Institute

Submitted
16 January 1951

SOURCES AND BIBLIOGRAPHY

1. Keller, L., Friedman, A., "Differential Equations for the Turbulent Motion of a Compressible Fluid". Proc. of the first Int. Congr. for appl. mech., Delft, 1925.

2. Kolmogorov, A. N. "The Local Structure of Turbulence in a Non-compressible Liquid in the Presence of High Reynolds Numbers", DAN SSSR, Volume 30, No 4, 1941.

3. Kolmogorov, A. N. "Diffusion of Energy in the Presence of Local Isotropic Turbulence", DAN SSSR, Volume 32, No 1, 1941.

4. Krasil'nikov, V. A. "The Effect of the Pulsations of the Atmospheric Refraction Factor Upon the Diffusion of Ultra-short Radio Waves", Isvestiya AN SSSR (Communications of the Academy of Sciences USSR), Geographical and Geophysical Series, Volume 13, No 1, 1949.

5. Krasilnikov, V. A. "Fluctuations of the Angle of Incidence in the Phenomena of the Twinkling of the Stars", DAN SSSR, (Reports of the Academy of Sciences USSR) Volume 65, No 3, 1949.

6. Yudin, M. I. "The Theory of Turbulence and Wind Structure and Its application to the Problem of the Oscillations of an Airplane in Flight", Gidrometizdat, 1946.

7. Obukhov, A. M. "The Distribution of Energy in a Turbulent Current Spectrum", Izv. AN SSSR (Communications of the

Academy of Sciences), Geographical and Geophysical Series, No 4-5, 1941.

8. Obukhov, A. M. "The Local Structure of Atmospheric Turbulence", DAN SSR (Reports of the Academy of Sciences), Volume 66, No 1, 1949.

9. Townsend, A. A. "Experimental Evidence for the Theory of Local Isotropy", Proc. Cambr. Phil. Soc., Volume 41, No 4, 1948.

10. Godecke. "Measurements of Atmospheric Turbulence", Annalen d. Hydrographic, H. 10, 1936.

11. Popov, S. G. "The Measurement of Air Currents", Gostekhizdat, 1947.

12. Obukhov, A. M. "Atmospheric Turbulence", Izv. AN SSSR (Communications of the Academy of Sciences USSR), Physical Series, Volume 6, No 1-2, 1942.

13. Krechmer, S. I. "The Experimental Determination of the Thermal Reluctance of the Thermoanemometer", DAN SSSR (Reports of the Academy of Sciences USSR), Volume 61, No 6, 1948.

14. Krechmer, S. I., Obukhov, A. M., Pinus, N. Z. "The Work of the Central Aerological Observatory", GUGMS, No 6, 1951.

15. Konstantinov, A. R. "Investigation of the Turbulent Structure of the Wind in the Lowest Atmospheric Layer", Works of the Central Geophysical Laboratory GUGMS, No 16 (78), 1949.

16. Reynolds, O. "On the Dynamical Theory of Incompressible Viscous Fluids", 1895. (A Russian translation of this article can be found in the Symposium "Problemy turbulentnosti" (Problems of Turbulence), ONTI, 1936).

17. Laykhtman, D. L. and Chudnovskiy, A. F. "The Physics of the Lowest Atmospheric Layer", Gostekhizdat, 1949.

E N D

APPENDIX ([illegible])

Фиг. 5. Раздвижная каретка для установки терм

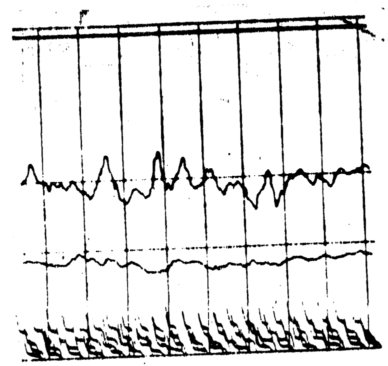

Фиг 6. Образец записи дифференциального термоанемометра (разность скоростей на базе 8 см)

Fig.6. [illegible] of differential [illegible] (difference of velocities on base of 8 cm)

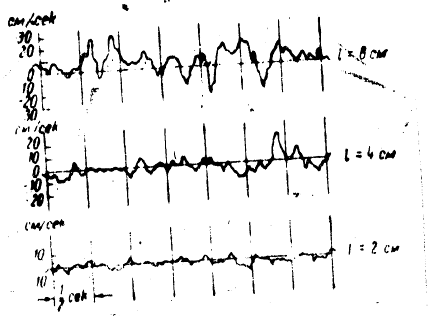

Фиг. 7. Разность скоростей ветра на расстояниях 2, 4, 8 см

Fig.7. Difference in wind velocities at distances of 2, 4, 8 cm.

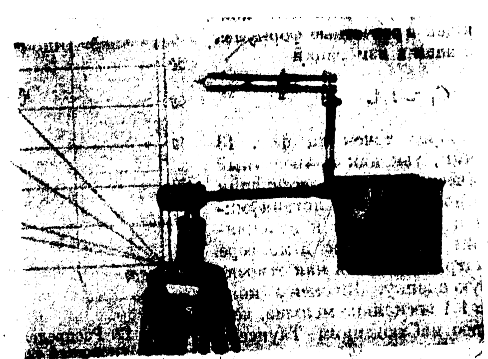

Фиг. 15. Флюгарка для углового насадка

Fig.15. [illegible] vane for the angular [illegible] fittings.

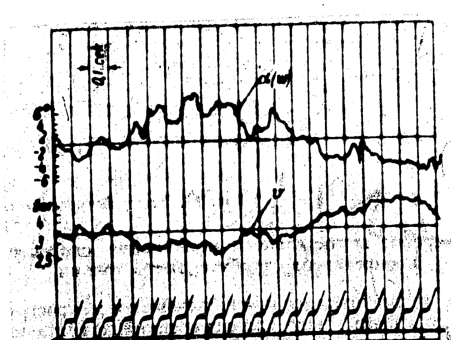

Фиг. 16. Образец регистрации вертикальной составляющей скорости ветра

Fig.16. Sample of recording of the vertical wind velocity component.

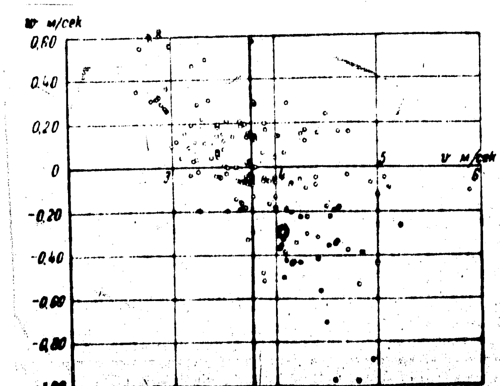

Фиг. 18. Корреляция горизонтальной и вертикальной составляющей скорости ветра

Fig.18. Correlation of horizontal and vertical wind velocity components.